Effects of Viscoelastic Properties on the Dielectric and Electrooptic Responses of Low-T_g Guest−Host Polymers

Jean-Charles Ribierre,*,† Loïc Mager,† Alain Fort,† and Stéphane Méry‡

IPCMS, Groupe d'Optique Non Linéaire et d'Optoélectronique, Matériaux Organiques pour l'Optique Nonlinéaire, and IPCMS, Groupe des Matériaux Organiques, CNRS UMR 7504, 23, rue du Loess, 67037 Strasbourg Cedex, France

Received August 2, 2002; Revised Manuscript Received January 30, 2003

ABSTRACT: The dynamics of the electrooptic and dielectric properties in low-T_g photorefractive guest−host polymers are directly related to the orientational dynamics of doping nonlinear optical chromophores. We report on experimental results on the orientational mechanisms of chromophores above T_g, investigated by ellipsometry and dielectric spectroscopy. These measurements have been performed on plasticized poly(*N*-vinylcarbazole) and polysiloxane functionalized with a carbazole pendant, doped with nonlinear optical chromophores. The data are compared to the mechanically measured complex shear compliance of the materials. The results of this comparison demonstrate that the orientational dynamics of chromophores are entirely ruled by the viscoelastic properties of the polymer matrix. In addition, the influence of the chromophore size is investigated and interpreted by using free volume and rheological laws. Finally, the evidence of an anelastic memory, induced by the orientation of the chromophores below T_g, is pointed out.

I. Introduction

Photorefractivity appears in materials that simultaneously exhibit generation, transport, and trapping of charges as well as electrooptical (EO) properties. This effect was observed for the first time in polymeric materials in 1991.[1,2] Low glass transition temperature (T_g) photorefractive (PR) doped polymers are a mixture of a photoconductive polymer host, a photosensitizer, and push−pull chromophores. Further developments of new and more efficient photorefractive polymers require an optimization of the individual component properties enlightened by a full understanding of their mutual interactions. For this purpose, most of the recent studies have been essentially devoted to the photoconductive properties of polymer hosts[3−5] and to the nonlinear optical (NLO) properties of chromophores.[6−8] Here, we focus our attention on the mechanical interactions between chromophores and polymer hosts as well as the influence of the matrix on the orientational dynamics of chromophores.

To observe an EO effect in PR polymers, it is necessary to break the centrosymmetry by applying an external electric field, resulting in an orientation of the dipolar NLO molecules. The refractive index changes are induced by the Pockels effect related to the molecular quadratic hyperpolarizability $\beta(\omega)$ of the chromophores and by the orientational birefringence associated with the molecular linear polarizability anisotropy $\Delta\alpha(\omega)$ where ω is the light pulsation. It has been shown that this latter contribution is the most significant one for these materials. However, to observe the so-called orientational enhancement,[9] a high rotational mobility of the chromophores in the polymer host is required. For this purpose, polymers with T_g near room temperature, and consequently with a low viscosity, are generally used as a host. This low T_g can be an intrinsic property of the host or can be modified by incorporation of a plasticizer.

In these materials, the photorefractive response time depends not only on the photoconductivity but also on the EO effect. Previous works have demonstrated the influence of T_g on these properties and on the dynamics of the photorefractive effect.[10−14] However, the role played by the viscoelastic properties of the polymer matrix on the chromophore mobility is often neglected. The unique determination of T_g does not allow a complete description of the interactions between orientational dynamics of chromophores and polymer chain relaxation.

In this study, we investigate in details the orientational dynamics of chromophores by using dielectric spectroscopy and transmission ellipsometry setups on different doped polymers. The temperature dependence of their dielectric and electrooptic responses is directly compared to that of their shear compliance, determined at a macroscopic scale by using a mechanical rheometer. The shear compliance fully describes the viscoelastic behavior of polymers and provides information on the polymer chain dynamics. The analysis of the data presented here will demonstrate that the orientational dynamics of chromophores (orientation, relaxation, memory effect) are entirely dominated by the mechanical behavior of the materials. Besides, the same temperature dependencies of the dielectric, EO, and viscoelastic responses, observed in two different polymers doped with various chromophores, reveal the complete coupling between the orientational mobility of chromophores and the segmental polymer chain dynamics. The influence of the chromophore size on these processes is also investigated and described by introducing the local free volume theory. Finally, below T_g, the anelastic memory effects of the polymer matrix on the EO dynamics are characterized and explained by using the Boltzmann superposition principle.

II. Materials

The photoconductive polymer hosts used here are either the poly(*N*-vinylcarbazole) (PVK) or a polysiloxane functionnalized

† Groupe d'Optique Non Linéaire et d'Optoélectronique.
‡ Groupe des Matériaux Organiques.

10.1021/ma021246m CCC: $25.00
Published on Web 03/15/2003

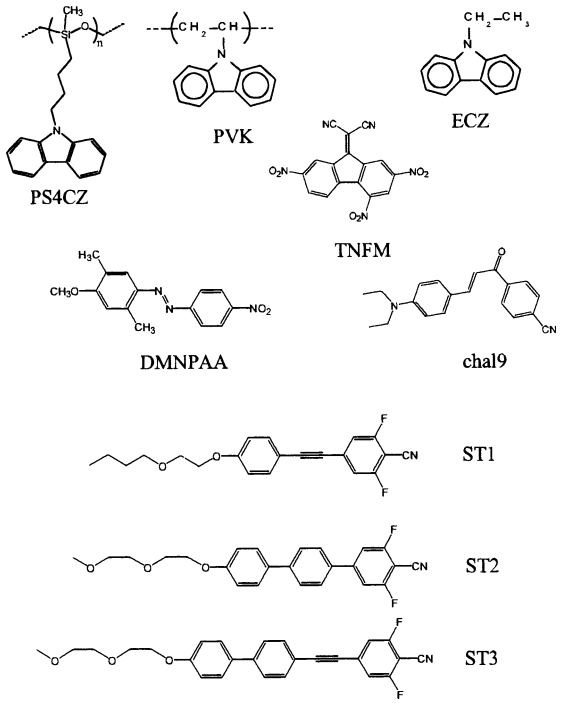

Figure 1. Chemical structures of the molecules.

with a carbazole pendant (PS4CZ) (see Figure 1) exhibiting respective T_g of 200 and 40 °C. For PVK-based composites, despite the plasticizing effect of doping chromophores, *N*-ethylcarbazole (ECZ) is added to lower T_g near room temperature. Besides, it has been previously shown that the incorporation of ECZ in PVK-based photorefractive composites improved the photoconductivity, the orientational mobility of the chromophores, and, finally, the photorefractive performances.[15,16] The composition of the materials and their corresponding T_g, determined by differential scanning calorimetry at a heating rate of 10 °C min^{-1}, are listed in Table 1. The variations of T_g between the pure and doped polymers illustrate the plasticizing effect of the chromophores on the polymer host. The chemical structures of the chromophores added to these polymers are shown in Figure 1. These push−pull molecules exhibit permanent dipole moments between 5 and 7 D as well as NLO properties. The absorption spectra of the 4-((*E*)-4-(4-diethylaminophenyl)-2-oxo-3-butenyl)benzonitrile (chal9) and 2,5-dimethyl-4-(*p*-nitrophenylazo)anisole (DMNPAA) show peaks located respectively at 440 and 395 nm and present a low absorption respectively above 550 and 600 nm. The ST1 (also called FTCN),[8] ST2, and ST3 chromophores are fully transparent in the visible range. Although no photorefractive measurements are performed in this work, the photosensitizer (2,4,7-trinitro-9-fluorenylidene) malonodinitrile (TNFM) is added to the doped polymers. The formation of a charge-transfer complex between TNFM and a carbazole pendant allows charge photogeneration and then photorefractivity in the visible region. All the low-T_g doped polymers considered in this work exhibit a photorefractive effect. This feature is significant, since our attention is focused here on the mechanical interactions between chromophores and polymer host in photorefractive doped polymers.

To prepare the samples, the different compounds are dissolved and well mixed in chloroform. Then, the mixtures are dried and placed in a vacuum oven at 90 °C for 12 h to eliminate the residual solvent. In the case of PVK-based materials, a mechanical homogenization is made at T_g + 75 °C to improve their optical quality. The materials are then sandwiched between two parallel indium tin oxide (ITO)-coated glass slides at T_g + 75 °C. Spacers of 105 μm are used to achieve a uniform sample thickness.

III. Experiment

Different experimental approaches can be used to probe the orientational dynamics of chromophores in guest−host polymers: the dielectric spectroscopy,[17] the second harmonic generation,[18−20] and the EO dynamics measurements.[21,22] In this work, we only use dielectric spectroscopy and ellipsometric techniques. These approaches do not have the same dependence toward the average orientation of the chromophores. Considering that the push−pull chromophores are rodlike molecules and, by introducing θ, the polar angle between the permanent dipole moment and the applied electric field directions, the dielectric and EO responses are respectively proportional to the orientational average functions $\langle\cos\theta\rangle$ and $\langle\cos^2\theta\rangle$. These expressions, which are equivalent to the first and the second moment of the time-dependent orientation autocorrelation function,[23] imply differences between the EO and dielectric response times as previously demonstrated.

Dhinojwala et al.[20] have shown the coupling between the orientational processes of chromophores and the polymer chain dynamics via EO, dielectric, and SHG dynamics experiments. It is well-known now that the orientational response times follow respectively above and below T_g the William−Landel−Ferry (WLF) and Arrhenius laws. However, the temperature dependencies have never been directly compared to that of their viscoelastic responses. A crucial point is that the incorporation of chromophores or other plasticizing molecules strongly modifies the viscoelastic properties of polymers, not only by a decrease of T_g but also by a change in the shape of their frequency-dependent compliance response curve. Mechanical characteristics such as the WLF coefficients of pure polymers, easily found in the literature, cannot be directly employed to analyze the behavior of the orientational dynamics of chromophores. In this work, we will present together EO, dielectric, and mechanical response measurements of our materials for temperatures between T_g and T_g + 50 °C. Consequently, these responses will be directly compared along several decades time scale. The results clarify the orientational processes of the chromophores and demonstrate that these processes are entirely coupled with the dynamics of the polymer chains.

Ellipsometric Measurements.[24,25] For this setup, we use a light source consisting of 1 mW laser diode emitting at a wavelength of 670 nm. The sample is positioned between two crossed polarizers and inclined at an incidence angle of 45°. The incident beam is linearly polarized at 45° of the incidence plane. A Soleil−Babinet−Bravais compensator placed between the sample and the analyzer enables the adjustment of the relative phase difference between the s and p polarizations of the laser beam in order to optimize the sensibility of the measurements. The light intensity is measured with a photodiode connected to a numeric oscilloscope or a lock-in amplifier. The refractive index variation Δn is related to the light beam intensity change ΔI by the following equation:[26]

$$\frac{\Delta I}{I_0} = \frac{\pi d}{\lambda G}\Delta n \qquad (1)$$

where I_0 is the incident intensity, d is the sample thickness, λ is the light wavelength, and G is a geometric factor equal to 4.6 in our experimental configuration.

Table 1. Physical Parameters of the Studied Doped Polymers[a]

	T_g (°C)	C_1^g	C_2^g (°C)	f_g	α_f (°C^{-1})	μ (D)
(PS4CZ:chal9) (80:20 wt %)	23	14.2	52	0.0305	5.9×10^{-4}	6.6
(PS4CZ:DMNPAA) (80:20 wt %)	29	13.2	52	0.0329	6.3×10^{-4}	5.6
(PS4CZ:ST1) (80:20 wt %)	10	13	52	0.0334	6.4×10^{-4}	
(PS4CZ:ST2) (80:20 wt %)	21.5	13.7	52	0.0317	6.1×10^{-4}	
(PS4CZ:ST3) (80:20 wt %)	18	14.7	52	0.0295	5.7×10^{-4}	
(PVK:ECZ:chal9) (40:40:20 wt %)	−7	11.6	62	0.0374	6×10^{-4}	6.5
(PVK:ECZ:ST1) (40:40:20 wt %)	−15	10.2	62	0.0423	6.8×10^{-4}	6.1
(PVK:ECZ:ST2) (40:40:20 wt %)	−7	10.9	62	0.0398	6.4×10^{-4}	5.3
(PVK:ECZ:ST3) (40:40:20 wt %)	−20	12.1	62	0.0359	5.8×10^{-4}	5

[a] The Williams−Landel−Ferry coefficients C_1 and C_2 are determined for a reference temperature, here chosen equal to T_g. The parameters f_g and α_f respectively correspond to the fractional free volume and the thermal expansion coefficient at T_g. μ is the permanent dipole moment of the chromophores.

Δn corresponds to the difference between the induced variations of the extraordinary and ordinary refractive indexes.

With this experimental setup, it is possible to investigate the time or frequency resolved EO responses of the samples. In the first case, a 2 kV voltage magnitude is applied across the sample. The orientational dynamics are analyzed by recording the EO responses either upon the application of the dc field or removal of the dc field. The buildup and the decay of these responses are directly monitored with an oscilloscope (Tektronix TDS 410A).

In the second case, a 1 kV sinusoidal ac voltage is superposed to a 1 kV dc voltage for frequency-resolved measurements. The high- and low-frequency limits of the ac field are respectively 4 kHz and 0.1 Hz. The light intensity variations at the ac voltage fundamental oscillation frequency Ω and at the second harmonic frequency 2Ω, as well as their respective differences of phase, are analyzed with a lock-in amplifier (EG&G instruments 7265). At high frequencies, the ac field effect on the chromophore orientation collapses due to a relatively high polymer matrix viscosity. In this frequency region, the EO response originates from the contribution of the quadratic hyperpolarizability only. At low frequencies, the chromophores can be oriented by the ac field, and the EO signal is then composed of both contributions of linear polarizability anisotropy and quadratic hyperpolarizability. Such a technique has been used to determine the microscopic parameters $\mu^2\Delta\alpha(\omega)$ and $\mu\beta(\omega)$, where μ is the chromophore permanent dipole moment, of the chromophores incorporated in the polymer host.[27]

To characterize the influence of the viscoelastic properties on the EO responses in these materials, the measurements are performed with the samples placed in an oven, where the temperature is controlled with a precision of 0.1 °C. As the viscosity of such materials is strongly dependent on the temperature, the measurements of time and frequency resolved EO dynamics performed at various temperatures will provide information on the relationships between the materials viscosity and the orientational dynamics of the chromophores.

Dielectric Spectroscopy. This technique provides information on the frequency and temperature dependence of the real and imaginary parts of the dielectric constant in polymeric systems. An impedance analyzer (Quad Tech 7400) is used in a frequency voltage domain ranging from 100 Hz to 500 kHz. These measurements are achieved by using the lumped circuit method in a parallel configuration.[28] The orders of magnitude for the measured capacity C and the resistance R of the samples are respectively a few pF and MΩ. The real part ϵ' and the imaginary part ϵ'' of the complex dielectric constant are given by

$$\epsilon' = \frac{C}{C_0} \qquad \epsilon'' = \frac{1}{R\Omega C_0} \tag{2}$$

C_0 is the capacity of the equivalent capacitor when the polymer is replaced by vacuum, and Ω corresponds to the oscillation frequency of the external electric field. Concerning all the materials considered in this work, the contribution of the ionic conductivity is very low in the experimental frequency and temperature ranges. The orientation of chromophores induced by the applied electric field generates an orientational polarization, which modifies ϵ' and ϵ''. Different formalisms have been previously developed to describe the dielectric behavior of such materials.[29−31] The Debye model cannot be used to characterize the dielectric response of doped polymers. It is more adequate for gaseous or low-viscosity liquid systems. The introduction of relaxation times distribution[32] is necessary for the description of the relaxations in polymers. In this work, the Havriliak−Negami (HN) equation, which can be viewed as a superposition of Debye processes, is employed:

$$\epsilon^*(\Omega) = \epsilon_\infty + \frac{\epsilon_s - \epsilon_\infty}{[1 + (i\Omega\tau)^{\alpha_{HN}}]^{\beta_{HN}}} \tag{3}$$

where τ is the dielectric relaxation time. Here, α_{HN} and β_{HN} are constant parameters related to the shape and the width of the relaxation times distribution whereas ϵ_s and ϵ_∞ are called the relaxed and unrelaxed values of the dielectric constant and correspond respectively to the values of ϵ' at low and high frequencies. The strength of relaxation ($\Delta\epsilon = \epsilon_s - \epsilon_\infty$) characterizes the macroscopic dipole moment induced by the orientation of the dipolar molecules along the direction of the external electric field. This parameter depends on the ground-state dipole moment μ of chromophores. The relationship between Δ and μ in polymeric systems has been established by Fröhlich:[33]

$$\epsilon_s - \epsilon_\infty = \frac{3\epsilon_s}{2\epsilon_s + \epsilon_\infty} \frac{4\pi N}{3k_b T}\left(\frac{\epsilon_\infty + 2}{3}\right)^2 g\mu^2 \tag{4}$$

where g is the Kirkwood correlation factor, which takes into account the orientational correlation between a reference molecule and its neighbors.

Viscoelastic Measurements. Rheometry involves the use of a precision actuator to apply onto a sample a slight, oscillatory, deforming shear stress. By using a sensitive transducer, we measure the strains generated

within the sample. Mechanical shear measurements are performed in this study by using a Rheometric Scientific ARES rheometer. Here, the material is placed in an oven between two parallel rotating plane plates. The measurements are carried out at temperatures ranging from 20 to 100 °C. The stress σ is here applied to the upper plate, and the induced strain is directly measured by a transducer connected to the lower plate. Dynamical mechanical analysis is a useful tool to simultaneously characterize the elastic and viscous material responses. The response can be computed and separated into two components: an elastic strain in phase with the applied stress and a viscous strain 90° out of phase with the stress. The mechanical response is then monitored and analyzed by a computer. By varying the polymer temperature, this technique enables a full description of the viscoelastic behavior of polymers.

To express the stress−strain relationship in such materials, it is necessary to introduce the complex shear compliance J^*.[34] The real part J' describes the material's ability to store elastic energy whereas the imaginary part J'' characterizes its ability to dissipate stress through heat. Our attention is focused here on the viscoelastic transition. It is in this region that the frequency dependence of viscoelastic properties is the most spectacular. Different models have been developed to describe this behavior. One of the simplest is the Voigt−Kelvin model, which only associates a Hookean spring and a dashspot in parallel. The frequency dependence of the storage J' and the loss compliance J'' is expressed by

$$J' \propto \frac{1}{1+\Omega^2\tau^2} \qquad J \propto \frac{\Omega\tau}{1+\Omega^2\tau^2} \tag{5}$$

where Ω is the oscillation frequency and τ is the retardation response time. This parameter corresponds to the ratio between the viscosity of the dashspot and the Young modulus of the spring. The Voigt−Kelvin model is sufficient here to characterize the viscoelastic behavior of doped polymers together with the estimation of the response times.

IV. Comparisons of the Temperature Dependence of the Dielectric, EO, and Viscoelastic Responses

A direct comparison is required between the viscoelastic, dielectric, and EO properties of doped polymers to characterize the influence of their mechanical properties on the orientational dynamics of chromophores. If the comparison between the dielectric and EO responses is quite straightforward, the connection with mechanical properties is much less evident. But we will see in the Results section that all the three different sets of measurements follow the time−temperature superposition principle.[34] In this context, the comparisons of those different properties can be then achieved through the WLF parameters.

In the frequency- and temperature-dependent measurements presented here, the curves have a similar shape and can be superposed, at a reference temperature, by a simple translation along the frequency axis, leading to the creation of a master curve. The temperature changes shift the time scale by several orders of magnitude due to the lowering of the polymer viscosity. The temperature dependence of the translation, or shift factor a_T, can be deduced from the formation of this master curve and is described by the WLF equation:[35]

$$\log a_T = \frac{-C_1(T-T_0)}{C_2+T-T_0} \tag{6}$$

The WLF coefficients C_1 and C_2 are characteristics of the polymer. They are respectively related to the fractional free volume f_0 and the thermal expansion coefficient α_f, as indicated by the following equations:

$$C_1 = \frac{1}{2.303 f_0} \qquad C_2 = \frac{f_0}{\alpha_f} \tag{7}$$

The fractional free volume f_0 corresponds to the relative difference between the total volume and the volume occupied by the molecules. These WLF parameters strongly depend on the reference temperature generally chosen in the literature equal to T_g. For another reference temperature T'_0, these parameters are calculated as

$$C'_1 = \frac{C_1 C_2}{C_2 + T'_0 - T_0} \qquad C'_2 = C_2 + T'_0 - T_0 \tag{8}$$

The WLF equation can be derived by considering the viscosity behavior in terms of free volume using the Doolittle equation:[34]

$$\eta = A \exp\left(B \frac{v - v_f}{v_f}\right) \tag{9}$$

where A and B are parameters related to the materials; v and v_f are respectively the specific volume and the free volume. It has been demonstrated that the temperature dependence of the orientational dynamics of the chromophores follows the WLF and Doolittle equations above T_g and an Arrhenius law below T_g. However, a direct comparison between EO, dielectric, and viscoelastic dynamics measurements has never been performed on the same doped polymers. Whereas the orientational processes of chromophores will be characterized at a microscopic scale by dielectric spectroscopy and ellipsometry measurements in several guest−host polymers, the viscoelastic properties of these materials will be described at a macroscopic level by the complex shear compliance measurements. This study not only will confirm the results previously reported but also will establish more precisely the mechanical interactions between chromophores and polymer hosts.

V. Results and Discussion

Frequency and temperature resolved ellipsometry measurements have been performed on (PS4CZ:chal9) (80:20 wt %), (PVK:ECZ:ST1) (40:40:20 wt %), and (PVK:ECZ:ST2) (40:40:20 wt %) films. Figure 2 shows the evolution of the second harmonic EO response for (PS4CZ:chal9), for frequencies varying from 0.1 Hz to 1 kHz and for temperatures between 27 and 45 °C. Plateaus are observed at low and high frequencies at Ω and 2Ω. However, for all PVK-based composites considered here, the plateau at low frequencies is not precisely defined, as shown in Figure 3. As a consequence, there is in this case in some uncertainty (≈10%) concerning the evaluation of the parameters reduced to zero frequency, $\mu^2\Delta(0)$ and $\mu\beta(0)$, in the two-level model approximation.[36] For ST1, ST2, and ST3, the $\mu^2\Delta(0)$

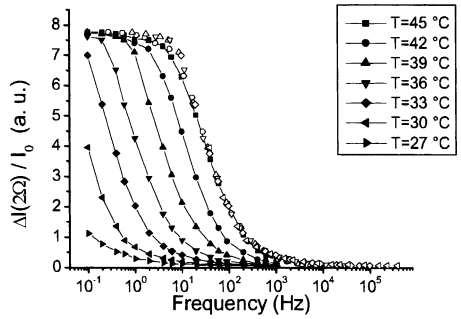

Figure 2. Frequency dependence of the electrooptical responses in (PS4CZ:chal9) (80:20 wt %) at different temperatures (solid symbols). Lines are guides for the eyes. A master curve (open symbols) is constructed at the reference temperature of 70 °C.

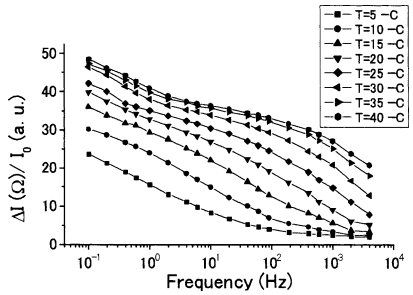

Figure 3. Frequency dependence of the electrooptical responses in (PVK:ECZ:chal9) (40:40:20 wt %) at different temperatures.

values determined by frequency-resolved ellipsometry are calculated neglecting the contribution due to $\mu\beta(0)$ as their quadratic hyperpolarizabilities measured by EFISH[36] are found to be very low. The data listed in Table 2 are little dependent on the polymer host and are consistent with those determined by EFISH and ellipsometry techniques in liquids.[37] The ST1, ST2, and ST3 molecules present a very strong linear polarizability anisotropy, a very low quadratic hyperpolarizability, and a high solubility in polymer. They have been specially synthesized for this purpose and are very good candidates for photorefractive doped polymers. All these materials exhibit a negligible contribution of the third-order nonlinear optical effects as shown by the response $\Delta I(2\Omega)/I_0$ at high frequencies.[27] Furthermore, the ratio of 4 predicted by the theory between $\Delta I(\Omega)/I_0$ and $\Delta I(2\Omega)/I_0$ at low frequencies is verified.

Whereas $\Delta I(\Omega)/I_0$ depends on the dc and ac fields, $\Delta I(2\Omega)/I_0$ is only function of the modulated field.[27] To characterize the influence of the temperature on the orientational dynamics of chromophores, we will consider essentially the second harmonic EO response to be in the same conditions as the dielectric and viscoelastic experiments where the external solicitations are purely sinusoidal and present no offset. However, the models proposed here may also describe the behavior of the first harmonic EO response. Figures 2 and 3 illustrate the strong influence of the temperature on the dynamics of the EO responses. A displacement of the isothermal curves to the high frequencies is observed with a temperature increase. It must be noticed that both plateaus are not simultaneously observed experimentally for the lowest and highest temperatures. This is due to respectively too high and too low viscosity, combined with a limited frequency experimental range. However, both plateaus are well present in these cases, as shown by the master curve.

The phase lags $\varphi(\Omega)$ and $\varphi(2\Omega)$ between the ac field and the EO responses have also been measured. Figure 4 shows the results obtained with (PS4CZ:chal9) (80:20 wt %) at 2Ω. At low and high frequencies, the EO responses and the applied voltage are in phase, a situation which corresponds to an elastic behavior. For the intermediate frequencies, a phase lag appears due to the viscoelastic transition of polymers. With the knowledge of the magnitude and the phase lag of the EO response, the *in-phase* and the *90° out-of-phase* components can be easily determined. These curves provide direct information on the chromophores mobility in the viscoelastic matrix, since a given frequency establishes a time scale where the ability of chromophore orientation can be observed. A large similitude between the EO responses and the typical mechanical responses is observed. As shown in Figure 5, fits of the *in-phase* and *90° out-of-phase* EO responses are obtained by using a Kelvin−Voigt type equation (eq 5). The location of the viscoelastic transition is estimated by the retardation time, which corresponds to the inverse of the frequency associated with the inflection point of the storage compliance and the maximum of the loss compliance peak. Similarly, the orientational dynamics of chromophores can be characterized by the EO response times obtained from the Voigt−Kelvin equation. The temperature dependence of the EO response times, τ_{EO}, follows the WLF equation. We want to compare the temperature dependence of the shift factor, a_T, deduced from the superposition of the EO response curves, to those obtained from dielectric and mechanical measurements. However, although the Voigt−Kelvin or Debye equations provide a good estimation of the orientational response times, the experimental real and imaginary parts of the EO response are broader than the corresponding fitting curves. This is a typical result obtained for the α-relaxation in polymeric systems.[28] This equation describes a relaxation with a single response time in the frequency space and corresponds in the temporal space to a single-exponential function. Since chromophores embedded in the polymer matrix have different microscopic surroundings, the orientational dynamics of chromophores exhibit a range of response times. Although the response times determined from the Debye and the HN equations are almost identical, this latter equation, which introduces the distribution functions, duplicates more accurately the frequency dependence of the EO response, as shown in Figure 5.

Dielectric measurements have been performed on several doped polymers. Figure 6 and Figure 7 show the real and the imaginary parts of the dielectric constant as a function of the temperature and the oscillation frequency for PS4CZ doped with chal9. A very good superposition of the isothermal curves is once again achieved by a simple translation along the frequency axis, similar to the EO responses. A very good fit of $\epsilon'(\omega)$ and $\epsilon''(\omega)$ is obtained by using the HN equation. The dielectric response times follow a WLF law and are consistent with the EO dynamics. The parameters α_{HN} and β_{HN} do not vary with the temperature, for all the studied doped polymers, in good agreement with the time temperature principle. Since the shape of curves is not affected by temperature changes, the relaxation time distributions must be invariant with temperature. It must be noticed that for all the samples $\epsilon''(\omega)$ only exhibits a α-relaxation peak. The experimental frequency range is probably not broad enough to observe

Table 2. Physical Parameters of the chal9, ST1, ST2, and ST3 Molecules[a]

	V_0, Å^3	$\mu^2\Delta(0)$,[a] esu	$\mu^2\Delta(0)$ in PVK,[b] esu	$\mu^2\Delta(0)$ in PS4CZ,[b] esu	$\mu\beta(0)$,[c] esu	$\mu\beta(0)$ in PS4CZ,[b] esu
chal9	308	6×10^{-58}	8×10^{-58}	4.5×10^{-58}	305×10^{-48}	347×10^{-48}
ST1	251	23×10^{-58}	32×10^{-58}	31×10^{-58}		
ST2	278	24×10^{-58}	24×10^{-58}	29×10^{-58}		
ST3	310	33×10^{-58}	25×10^{-58}	27×10^{-58}		
DMNPAA	263	14×10^{-58}			210×10^{-48}	

[a] These values are determined from (a) ellipsometry measurements in liquid, (b) ellipsometry measurements in films, and (c) EFISH. The volume of these molecules V_0 has been calculated by using their van der Waals volumes.

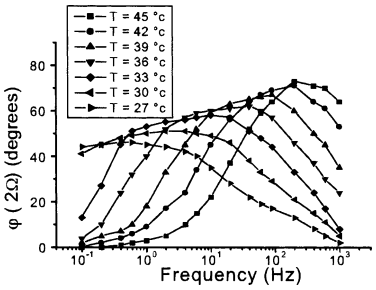

Figure 4. Influence of the temperature on the phase lag $\varphi(2\Omega)$ as a function of the oscillation frequency Ω in (PS4CZ:chal9) (80:20 wt %). Lines are guides for the eyes.

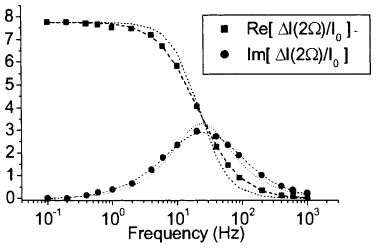

Figure 5. Frequency dependence of the *in-phase* and *90° out-of-phase* electrooptical responses at 45 °C in (PS4CZ:chal9) (80:20 wt %). The dotted line and the dashed line are fits deduced respectively from the Voig−Kelvin and Havriliak−Negami equation.

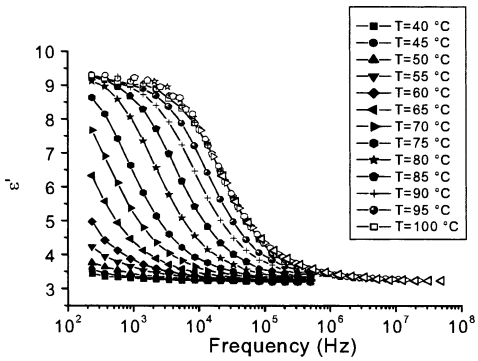

Figure 6. Frequency dependence of the real part of the dielectric constant ϵ' in (PS4CZ:chal9) (80:20 wt %) at different temperatures (solid symbols). A master curve (open symbols) is constructed at the reference temperature of 100 °C. Lines are guides for the eyes.

secondary relaxations. Besides, the β- and γ-relaxation peaks, which have been reported in previous studies,[38,39] are more generally observed for side chain polymers. The values of the chromophore dipole moment are given in Table 1, assuming that there are no chromophore−chromophore interactions ($g = 1$). The experimental value of the dipole moment of chal9 doping either PS4CZ or PVK was 6.5 ± 0.2 D, indicating a weak influence of the polymer hosts on the relaxation strength. To verify that the polymer hosts do not play a major role on the dielectric responses magnitude of doped polymers,

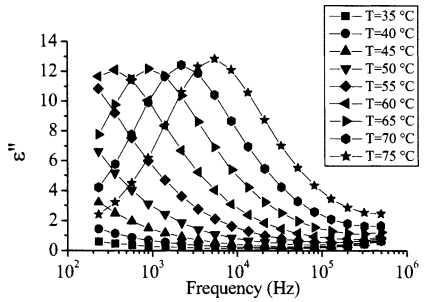

Figure 7. Frequency dependence of the imaginary part of the dielectric constant ϵ'' for PS4CZ doped with chal9 at different temperatures (solid symbols). Lines are guides for the eyes.

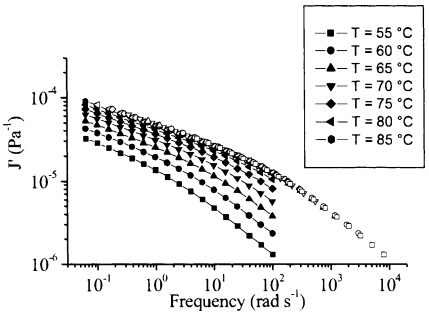

Figure 8. Frequency dependence of the storage compliance J' in (PVK:ECZ:ST2) (40:40:20 wt %) at different temperatures (solid symbols). A master curve (open symbols) is constructed at the reference temperature of 85 °C.

measurements have been performed on both pure polymers. In this case, the strengths of relaxation were negligible (<1%) compared to those obtained with doped materials.

Mechanical measurements have been carried out on several doped polymers in the linear range of the polymer viscoelastic responses. This linearity is verified by checking that the measured values of the storage and loss compliances are independent of the strain amplitude variation. The measured storage compliance obtained with (PVK:ECZ:ST2) (40:40:20 wt %) is reported in Figure 8. The shape of the experimental curves and the values of the loss and storage compliances show that only the viscoelastic relaxation is probed. The glassy and rubbery zones are not observed in the experimental frequency and temperature ranges. Almost 10 frequency decades are typically needed at a constant temperature to explore these different regions. Since the glassy and rubbery regions are not precisely revealed, it is not possible to fit precisely the experimental data with the Voigt−Kelvin equation. However, the creation of a master curve is achieved. Consequently, although the mechanical relaxation times are not accessible with our experimental measurements, their temperature dependence is determined from the superposition of the curves.

The temperature dependencies of the shift factors a_T deduced from the mechanical, dielectric, and EO mea-

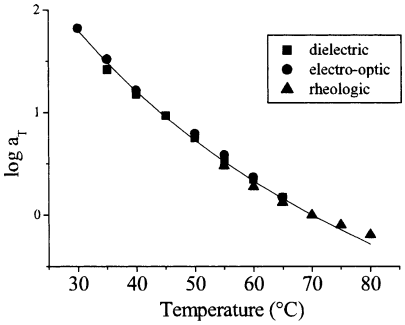

Figure 9. Temperature dependence of the shift factor a_T determined from dielectric, electrooptical, and mechanical measurements with a reference temperature of 70 °C in (PVK:ECZ:ST2) (40:40:20 wt %). These data are fitted by the Williams−Landel−Ferry equation.

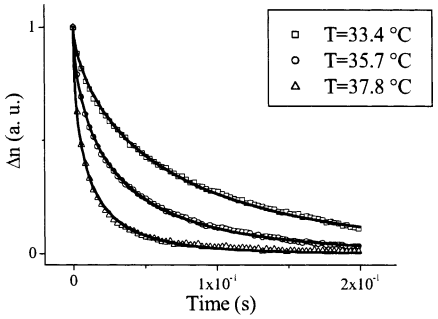

Figure 10. Temporal decays of the normalized electrooptical responses at several temperatures above T_g in (PS4CZ:chal9) (80:20 wt %). The applied electric field is turned off at $t = 0$. Curves are fitted with the Kohlrausch−Williams−Watts equation.

surements are compared for various doped polymers. The results obtained with (PVK:ECZ:ST2) (40:40:20 wt %) are shown in Figure 9. The experimental data measured by the three methods give the same WLF coefficients with a good approximation. The temperature dependence of the orientational dynamics of chromophores probed at a microscopic scale is identical to that of the bulk mechanical properties measured at a macroscopic level. This behavior clearly demonstrates that these orientational processes are entirely ruled by the viscoelastic properties of polymers and that, at a molecular level and above T_g, they are entirely correlated to the relaxation of cooperative segmental motions of polymer chains, in agreement with results previously reported by Dhinojwala et al.[40]

From this set of measurements, the WLF coefficients are determined for all the doped polymers studied up until now (see Table 1). The estimated uncertainties on these coefficients are more important in the PVK-based composites (≈12%) than in the doped PS4CZ (≈4%). To compare the various data, it is necessary to use eq 8 in order to take the reference temperature equal to T_g. C_1 varies not only with the polymer hosts but also with the chromophores. These results demonstrate not only that T_g plays a major role on these processes, in agreement with previous studies,[41,42] but also that the temperature dependence of the orientational dynamics changes with the polymer hosts and with the chromophores The C_1 value is useful here for the characterization of the rotational mobility of chromophores in the polymer host without any direct comparison of response times. The rotational motion of chromophores can be restricted below T_g when the size of the local free volume is not sufficient, respecting that of the chromophores. Liu et al.[19] have evaluated an apparent mean free volume, where the NLO molecules can rotate in a first-order approximation, and have expressed it as a function of the chromophore size. They have considered that the rodlike NLO molecules wobble around their geometrical center within two cones. Besides, Hampsch et al.[43] have demonstrated that below T_g the orientational dynamics of chromophores were affected by physical aging and dopant size. As the mobility of the chromophores is sensitive to the local free volume available in the polymer host, the smallest chromophores require less free volume for reorientation. However, the chromophore size affects also the mobility of chromophores above T_g. For this purpose, the chromophore volumes were calculated using their van der Waals volumes and are given in Table 2. A decrease of the fractional free volume deduced from the values of C_1 is observed when the doping molecule volume increases for PS4CZ- and PVK-based composites. However, to characterize more accurately the influence of the chromophore size on these orientational processes, the temperature dependence of orientational response times must be directly investigated on polymers doped by chromophores with various sizes.

Various methods are used to evaluate the orientational response times of chromophores in doped polymers. From frequency-resolved experiments, the dielectric, EO, and mechanical data are fitted by HN equation leading to the determination of the response times. Previous studies[32,44,45] have shown the relationship between the HN equation and the stretched exponential or Kohlrausch−Williams−Watts (KWW) equation,[46] commonly used to describe orientational processes in the temporal domain. The decay and buildup of the induced birefringence as well as the second harmonic generation signal at a constant temperature exhibit a non-single-exponential relaxation and are fitted by using the KWW equation:

$$y = \exp\left[-\left(\frac{t}{\tau}\right)^{\beta_{kww}}\right] \qquad 0 < \beta_{kww} \leq 1 \tag{10}$$

y is the relaxation parameter of interest, τ is the response time, and β_{kww} is the stretching parameter, which is related to the response times distribution breadth. An average orientational response time $\langle\tau\rangle$ is generally introduced as follows:

$$\langle\tau\rangle = \frac{\tau\,\Gamma(1/\beta_{kww})}{\beta_{kww}} \tag{11}$$

where Γ is the gamma function. The use of this method is sufficient to show a quantitative relationship between the polymer segment dynamics and the temporal behavior of the induced birefringence. The temporal decay and buildup of the EO responses have been monitored and analyzed for different temperatures in several doped polymers. The average response times of EO decays $\langle\tau_d\rangle$ and EO rises $\langle\tau_r\rangle$ are in good agreement with those found in frequency-resolved ellipsometry. The temporal EO decays obtained in (PS4CZ:chal9) (80:20 wt %) at different temperatures are shown in Figure 10. It directly illustrates the strong influence of the temperature on the orientational dynamics of chromophores. The stretching parameter β_{kww}, which is equal to 0.68 ± 0.02 for all the doped PS4CZ and to 0.75 ± 0.03 for all the doped PVK, does not change with the temperature, in agreement with the time−temperature

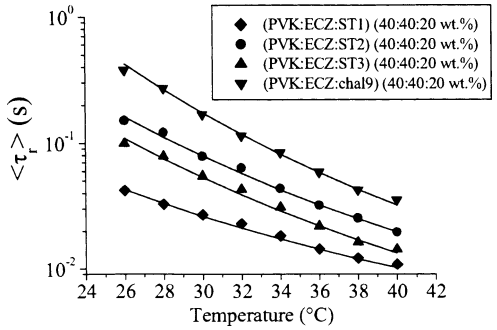

Figure 11. Temperature dependence of rise response times in PVK based guest−host polymers doped with different chromophores. The data are fitted with a Williams−Landel−Ferry equation taking a reference temperature of 36 °C.

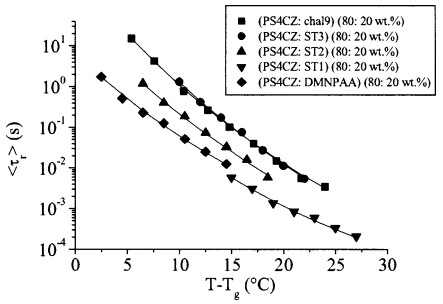

Figure 12. Temperature dependence of the rise response times in PS4CZ doped at 20 wt % for different chromophores. The data are fitted with the Williams−Landel−Ferry equation.

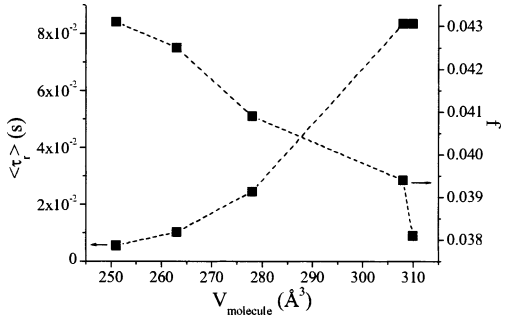

Figure 13. Orientational response times (square) and fractional free volume (triangle) at $T = T_g + 15$ °C plotted vs the chromophore volume in PS4CZ.

superposition principle but in contradiction with results previously reported.[47,48] A ratio of 3 is found between τ_d and τ_r, independent of the temperature.[49] The temperature dependence of these response times follows the WLF equation, in good agreement with the results obtained from frequency-resolved ellipsometry. Figure 11 shows the different values of $\langle\tau_r\rangle$ obtained for several doped polymers as a function of the temperature. The WLF coefficients have been determined from the fit of these data, and their values are indicated in Table 1. The differences, which appear between these response times, are due not only to the variation of T_g with the incorporated chromophores but also to the size of these molecules. For this purpose, the EO response rise times measured on doped PS4CZ are reported in Figure 12. They are plotted vs $T - T_g$ in order to suppress the role of T_g on the orientational dynamics and are fitted by the WLF equation. A variation of 4 orders of magnitude in the response times has been found between $T_g + 5$ and $T_g + 25$ °C in the case of PS4CZ doped with chal9. This property well demonstrates the major role played by the temperature on these processes. The shortest orientational response times are obtained with ST1 molecule, in good agreement with results previously reported by Kippelen et al.[8] They measured very short photorefractive response times, of the order of 4 ms with PVK plasticized with ECZ and doped with ST1 molecule. Furthermore, these data illustrate clearly the role of the dopant size in regard to the volume of the molecules. Indeed, plotted vs $T - T_g$, the shortest orientational response times are obtained with the smallest chromophores, which confirms the results previously reported in this work. Figure 13 shows the chromophore volume dependence of the orientational response times at $T - T_g$=15 °C in PS4CZ. The Doolittle equation cannot be directly used here since the free volume varies with the different chromophores. No simple relationships can be established between the fractional free volume or the orientational response times and the chromophore size since the free volume introduced by chromophores is not predictable. Besides, this free volume is not additive with that of the polymer matrix.[34] As expected, an increase of response times is associated with a decrease of fractional free volume. However, the role of T_g is of great consequence on the performances. It can be seen in Table 1 that a polymer doped with the same amount of different chromophores can exhibit very different T_g: for example, a variation of 11.5 °C is observed in the value of T_g between (PS4CZ:ST1) (80: 20 wt %) and (PS4CZ:ST2) (80:20 wt %). Consequently, at a given temperature, whereas, plotted against $T - T_g$, ST1 is reoriented approximately 4 times more quickly than ST2, a difference of 3 orders of magnitude in response times is obtained when plotted against the temperature.

All the previous results have been realized at a temperature above T_g. We have shown that the temperature dependence of the EO, dielectric, and mechanical properties are described by the same WLF law between T_g and $T_g + 100$ °C. Other studies[50−52] have clearly demonstrated that below T_g these properties follow an Arrhenius law with an activation energy varying with the considered polymer. Kuzyk et al. have developed a technique to estimate the elastic constant by SHG measurements and have compared the calculated molecular elasticity with the measured elastic modulus.[53,54] In this way, they have shown the influence of the matrix elasticity on the orientational dynamics of chromophores. Whereas the effects of mechanical memory are not very significant above T_g, they are omnipresent near and below T_g and play a major role in the orientational processes of chromophores.[55] Measurements have been performed on (PS4CZ:chal9) (80: 20 wt %) to prove such phenomena. Below T_g, at 19.3 °C, the temporal evolution of the induced birefringence has been monitored during five successive voltage pulses of 1800 V (Figure 14). When a constant electric field is applied across doped polymers, the EO response can be divided into distinct regions similar to the typical mechanical responses.[34] For a linear viscoelastic material, the total strain induced in a creep experiment is the sum of three contributions: an immediate elastic deformation, a viscoelastic deformation, and an unrecoverable Newtonian flow. Consequently, when an applied stress is removed, a polymer does not relax to the initial state due to this latter contribution. Figure 14 illustrates such behavior. The instantaneous EO contributions, which are observed during the buildup and the decay, can be attributed to an elastic deformation

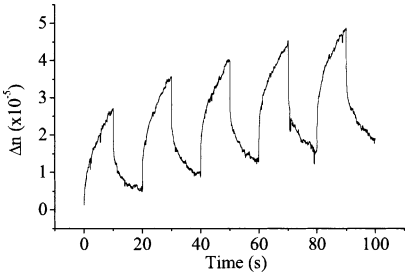

Figure 14. Electrooptical response for successive pulses of voltage applied across (PS4CZ:chal9) (80:20 wt %) at 19.3 °C.

of the polymer matrix induced by the reorientation of chromophores. The regions related to viscoelastic and anelastic deformations of the matrix are also clearly shown. It is important to notice that below T_g the orientation of the chromophores does not relax back to the initial state because of the anelastic behavior. This EO response can be interpreted by using the Boltzmann superposition principle.[34] According to this principle, the effects of mechanical history are linearly additive. For a sequence of different finite stresses σ_i applied at a time $t = t_i$, the temporal evolution of the induced strain $\gamma(t)$ can be expressed by

$$\gamma(t) = \sum_{t_i=-\infty}^{t_i-t} \sigma_i J(t - t_i) \qquad (12)$$

The EO behavior shown in Figure 14 illustrates this principle since a superposition of single EO responses is obtained. Besides, a decrease of the orientational response times with the number of applied pulses is observed. The main origin of this effect is the accumulation of anelastic strains in the polymer host during each pulse. When the electric field is applied and removed several times successively, the chromophores induce a strain of the polymer host and consequently an enhancement of free volume during their orientations. This variation of free volume implies that the dopants have a greatest freedom of rotation after each pulse of voltage and can be aligned more quickly along the electric field direction. Such an effect has also been observed in other guest−host polymers. It will be necessary to take into account this phenomenon, which can be responsible for hologram cross-talk, in further study devoted to hologram recording in photorefractive guest−host polymers.

In summary, this work devoted to the orientational dynamics of chromophores shows that these orientational processes probed at a microscopic scale are entirely ruled by the viscoelastic properties of the polymer matrix characterized at a macroscopic level. The EO, dielectric, and viscoelastic properties of guest−host polymers are found to exhibit the same temperature dependence and follow the WLF equation. This behavior confirms the coupling between the orientational dynamics of chromophores and the polymer chain dynamics. These results open a new axis of optimization for the photorefractive doped polymer performances. It has been demonstrated that short orientational response times are obtained with polymers exhibiting fast mechanical dynamics. For this purpose, a polymeric matrix with a high elasticity and a low viscosity, such as an elastomer, could be employed. These materials are known to exhibit retardation times much shorter than those typically obtained with linear polymers. Besides, the electrical breakdowns are less likely to be observed in such materials than in amorphous polymers. However, their elaboration, and especially the incorporation of chromophores with a high concentration, should require much attention. The use of polymers with a low average molecular weight seems also interesting as shown by considerable work on molecular glass.[56−58] The average molecular weight plays a major role in the rheological properties of polymers. Below a critical weight characteristic of the polymer, there are no entanglements between polymer chains. In this case, the local viscosity and T_g strongly decrease with the molecular weight. Varying this parameter could be an interesting alternative to the incorporation of plasticizer. Preliminary measurements performed on polystyrenes with different molecular weight have confirmed this purpose. Besides, the polymer photoconductivity, which depends on T_g, should be improved by a molecular weight decrease. Previous works have shown that the photoconductivity in PVK becomes higher for a low molecular weight.[59] However, photoconductivity measurements have to be carried out to characterize precisely such behavior and to validate our suggestions.

VI. Conclusion

We have demonstrated that the orientational dynamics of chromophores are entirely correlated to the mechanical properties of the matrix in low-T_g photorefractive guest−host polymers. The EO and dielectric behaviors of such materials are well described by usual polymer rheology laws. The temperature dependence of these properties explained by the WLF equation proves that these orientational processes are entirely coupled with the polymer chains relaxation. Whereas the magnitude of the refractive index induced variations depends on the applied electric field magnitude, we have shown that the EO dynamics do not depend on this parameter because of the coupling between chromophore orientation and polymer relaxation. The role of the dopant size has also been investigated and analyzed by using the concept of free volume. Finally, we have verified that the polymer matrix has a mechanical memory which influences these orientational processes. This study devoted to the orientational dynamics of chromophores in low-T_g photorefractive guest−host polymers has established the different factors playing a major role in the EO and dielectric properties. It demonstrates that rheological properties of polymers have to be taken into account for further studies devoted to the elaboration and optimization of new photorefractive guest−host polymers.

References and Notes

(1) Ducharme, S.; Scott, J. C.; Twieg, R. J.; Moerner, W. E. *Phys. Rev. Lett.* **1991**, *66*, 1846.

(2) Schildkraut, J. S. *Appl. Phys. Lett.* **1991**, *58*, 340.

(3) Hendrickx, E.; Zhang, Y.; Ferrio, K. B.; Herlocker, J. A.; Anderson, J.; Armstrong, N. R.; Mash, E. A.; Persoons, A. P.; Peyghambarian, N.; Kippelen, B. *J. Mater. Chem.* **1999**, *9*, 2251.

(4) Däubler, T. K.; Bittner, R.; Meerholz, K.; Cimrova, V.; Neher, D. *Phys. Rev. B* **2000**, *61*, 20, 13515.

(5) Hofmann, U.; Grasruck, M.; Leopold, A.; Schreiber, A.; Schloter, S.; Hohle, C.; Strohriegl, P.; Haarer, D.; Zilker, S. J. *J. Phys. Chem. B* **2000**, *104*, 3887.

(6) Hendrickx, E.; Wang, J. F.; Maldonado, J. L.; Volodin, B. L.; Sandalphon, Mash, E. A.; Persoons, A.; Kippelen, B.; Peyghambarian, N. *Macromolecules* **1998**, *31*, 734.

(7) Fort, A.; Muller, J.; Mager, L. *Chem. Phys.* **1999**, *243*, 115.

(8) Kippelen, B.; Hendrickx, E.; Ferrio, K. B.; Herlocker, J.; Zhang, Y.; Peyghambarian, N.; Marder, S. R.; Anderson, J. N.; Armstrong, R.; Mery, S. *J. Imaging Sci. Technol.* **1999**, *43*, 405.
(9) Moerner, W. E.; Silence, S. M.; Hache, F.; Bjorklund, G. C. *J. Opt. Soc. Am. B* **1994**, *11*, 320.
(10) Swedek, B.; Cheng, N.; Cui, Y.; Zieba, J.; Winiarz, J.; Prasad, P. N. *J. Appl. Phys.* **1997**, *82*, 5923.
(11) Bittner, R.; Bräuchle, C.; Meerholz, K. *Appl. Opt.* **1998**, *37*, 2843.
(12) Binks, D. J.; West, D. P. *Appl. Phys. Lett.* **2000**, *77*, 1108.
(13) Blinks, D. J.; Khand, K.; West, D. P. *J. Opt. Soc. Am. B* **2001**, *18*, 308.
(14) Ribierre, J. C.; Cheval, G.; Huber, F.; Mager, L.; Fort, A.; Muller, R.; Méry, S.; Nicoud, J. F. *J. Appl. Phys.* **2002**, *91*, 1710.
(15) Bolink, H. J.; Krasnikov, V. V.; Malliaras, G. G.; Hadziioannou, G. *J. Phys. Chem.* **1996**, *100*, 16356.
(16) Bittner, R.; Däubler, T.; Neher, D.; Meerholz, K. *Adv. Mater.* **1999**, *11*, 123.
(17) Köhler, W.; Robello, D. R.; Willand, C. S.; Williams, D. J. *Macromolecules* **1991**, *24*, 4589.
(18) Wang, C. H.; Gu, S. H.; Guan, H. W. *J. Chem. Phys.* **1993**, *99*, 5597.
(19) Liu, L. Y.; Ramkrishna, D.; Lackritz, H. S. *Macromolecules* **1994**, *27*, 5987.
(20) Dhinojwala, A.; Hooker, J. C.; Torkelson, J. M. *J. Non-Cryst. Solids* **1994**, *172−174*, 286.
(21) Hooker, J. C.; Burghardt, W. R.; Torkelson, J. M. *J. Chem. Phys.* **1999**, *111*, 2779.
(22) Blink, D. J.; West, D. P. *J. Chem. Phys.* **2001**, *115*, 1060.
(23) Wang, C. H.; Pecora, R. *J. Chem. Phys.* **1980**, *72*, 5333.
(24) Teng, C. C.; Man, H. T. *Appl. Phys. Lett.* **1990**, *56*, 1734.
(25) Schildkraut, J. S. *Appl. Opt.* **1990**, *29*, 2839.
(26) Kippelen, B.; Sandalphon; Meerholz, K.; Peyghambarian, N. *Appl. Phys. Lett.* **1996**, *68*, 1748.
(27) Sandalphon; Kippelen, B.; Meerholz, K.; Peyghambarian, N. *Appl. Opt.* **1996**, 35, 14, 2346.
(28) McCrum, N. G.; Read, B.; Williams, G. *Anelastic and Dielectric Effects in Polymeric Solids*; Wiley: New York, 1967.
(29) Debye, P. *Polar Molecules*; Lancaster: Lancaster, PA, 1929.
(30) Jonscher, A. K. *J. Mater. Sci.* **1981**, *16*, 2037.
(31) Havriliak Jr., S.; Negami, S. *J. Polym. Sci., Part C* **1966**, *14*, 99.
(32) Alvarez, F.; Alegria, A.; Colmenero, J. *Phys. Rev. B* **1991**, *44*, 7306.
(33) Frohlich, H. *Theory of Dielectric*, 2nd ed.; Oxford University Press: Oxford, 1958.
(34) Ferry, J. D. *Viscoelastic Properties of Polymers;* Wiley: New York, 1961.
(35) Williams, M. L.; Landel, R. F.; Ferry, J. D. *J. Am. Chem. Soc.* **1955**, *77*, 3701.
(36) Oudar, J. L. *J. Chem. Phys.* **1977**, *67*, 446.
(37) Fort, A.; Muller, J.; Cregut, O.; Mager, L.; Vola, J. P.; Barzoukas, M. *J. Appl. Phys.* **1998**, *83*, 2888.
(38) Saez-Torres, P.; Sanchis, M. J.; Diaz-Calleja, R.; Guzman, J.; Riande, E. *J. Appl. Phys.* **2000**, *88*, 1593.
(39) Du Lei, Runt, J.; Safari, A.; Newnham, R. E. *Macromolecules* **1987**, *20*, 1797.
(40) Dhinojwala, A.; Wong, G. K.; Torkelson, J. M. *J. Chem. Phys.* **1994**, *100*, 6046.
(41) Hall, D. B.; Dhinojwala, A.; Torkelson, J. M. *Phys. Rev. Lett.* **1997**, *79*, 103.
(42) Strutz, S. J.; Hayden, L. M. *J. Polym. Sci., Part B* **1998**, *36*, 2793.
(43) Hampsch, H. L.; Yang, J.; Wong, G. K.; Torkelson, J. M. *Polym. Commun.* **1989**, *30*, 40.
(44) Dias, C. J. *Phys. Rev. B* **1996**, *53*, 14212.
(45) Alvarez, F.; Alegria, A.; Colmenero, J. *Phys. Rev. B* **1993**, *47*, 125.
(46) Williams, G.; Watts, D. C. *Trans. Faraday Soc.* **1970**, *66*, 80.
(47) Ghebremichael, F.; Kuzyk, M. G. *J. Appl. Phys.* **1995**, *77*, 2896.
(48) Singer, K. D.; King, L. A. *J. Appl. Phys.* **1991**, *70*, 3251.
(49) Wu, J. W. *J. Opt. Soc. Am. B* **1991**, *8*, 142.
(50) Dureiko, R. D.; Schuele, D. E.; Singer, K. D. *J. Opt. Soc. Am. B* **1998**, *15*, 338.
(51) Shuto, Y.; Amano, M. *J. Appl. Phys.* **1996**, *79*, 4358.
(52) Dhinojwala, A.; Wong, G. K.; Torkelson, J. M. *Macromolecules* **1993**, *26*, 5943.
(53) Kuzyk, M. G.; Singer, K. D.; Zahn, H. E.; King, L. A. *J. Opt. Soc. Am. B* **1989**, *6*, 742.
(54) Dirk, C. W.; Devanathan, S.; Velez, M.; Ghebremichael, F.; Kuzyk, M. G. *Macromolecules* **1994**, *27*, 6167.
(55) Schussler, S.; Richert, R.; Bassler, H. *Macromolecules* **1994**, *29*, 1266.
(56) Lundquist, P. M.; Wortmann, R.; Geletneky, C.; Twieg, R. J.; Jurich, M.; Lee, V. Y.; Moylan, C. R.; Burland, D. M. *Science* **1996**, *274*, 1182.
(57) Wang, L.; Zhang, Y.; Wada, T.; Sasabe, H. *Appl. Phys. Lett.* **1996**, *69*, 728.
(58) Zhang, Y.; Wang, L.; Wada, T.; Sasabe, H. *Appl. Phys. Lett.* **1997**, *70*, 2049.
(59) Blythe, A. R. *Electrical Properties of Polymers*; Cambridge University Press: New York, 1979.

MA021246M